Design of dynamically isotropic modified Gough- Stewart platform using a geometry-based approach

Yogesh Pratap Singh[1], Nazeer Ahmad[2], Ashitava Ghosal[1]

[1] Indian Institute of Science, Bangalore, India
[2] ISAC, Indian Space Research Organization, Bangalore, India

Abstract. A dynamically isotropic mechanism is useful for vibration isolation since such a mechanism can be used to attenuate the first six modes of vibration effectively and equally from a sensitive payload. A Gough-Stewart Platform (GSP) has been proposed, in literature, for six component vibration isolation. The conventional GSP, however, fails to give a dynamic isotropy; hence a Modified Gough-Stewart Platform (MGSP) is considered in this work. The force transformation matrix, together with a geometry-based approach, is used to obtain closed-form analytical solutions for dynamic isotropy in an MGSP. The more general case of variation of the centre of mass (COM) of the payload from the top platform is considered. The geometric approach presented in this work is easier, faster, and more systematic than the previously existing methods. The configurations obtained with the above approach were successfully validated with the simulation results obtained using ANSYS®.

Keywords: Modified Gough-Stewart Platform (MGSP), Dynamic isotropy, Natural frequency matrix, Force transformation matrix

1 Introduction

Several researchers have explored Stewart platform-based vibration isolator to attain desired micro-vibration isolation in spacecraft [1]. For effective vibration isolation, one of the primary design considerations is that the first six natural frequencies (translational and rotational) be nearly the same or ideally equal [1]. In such an ideal design, the first six modes (which contain a majority of the vibration energy) can be equally and effectively attenuated, thereby significantly reducing the vibration levels at the payload typically mounted on the top platform of a Stewart platform. In robotics literature, this condition is known as 'dynamic isotropy'. From a vibration isolation standpoint, if there is dynamic isotropy, all the peaks corresponding to the different degrees of freedom (DOF) would be very close to each other in the amplitude versus frequency curve. As a consequence, the vibration isolation of one DOF does not interfere with that of another DOF and destroys the overall isolator's isolator performance.

Several researchers have worked on the geometric, stiffness, force, and velocity isotropies [1-7]. Unfortunately, the response of the control system cannot be evaluated by these performances [2]. Additionally, a dynamically isotropic Stewart platform can not only simplify controls but also give information about stability, the lowest value of the natural frequency plays a crucial role in dynamic stability [3]. Dynamic isotropy or ensuring all-natural frequencies to be nearly equal also implies that we maximize the lowest natural frequency, which is a favorable criterion for stability [3]. Also, the coupling among all the six DOFs of the Stewart platform complicates the controller design leading to a reduction in control accuracy [4]. Dynamic isotropy will also ensure that we can use decoupled controllers because a MIMO system is ideally converted into a SISO system. These added advantages of dynamic isotropy over other types of isotropies are due to its dependence on the payload's mass centre and inertia properties along with the geometric and stiffness parameters.

A considerable amount of effort has been invested in studying various isotropies in a standard 6 x 6 GSP [1,3,6] leading to the conclusion that the dynamic isotropy for a standard GSP is not practically feasible due to the practical restriction in satisfying the inertia conditions $I_{ZZ} = 4I_{XX} = 4I_{YY}$ [2,5]. Pertaining to the above constraint, few researchers studied the isotropic conditions for a Modified Gough–Stewart Platform (MGSP) [2,5,7]. In MGSP, the attachment points are on two radii on the top and bottom platform instead of a single radius in the conventional case (see Fig. 1(a)). Jiang et al. [5] described an MGSP using a pair of hyperboloids and investigated dynamic isotropy conditions. Yao et al. [6] explored spatial isotropy configuration for a MGSP based force sensor using a Jacobian matrix. Yi et al. [7] also introduced a two-parameter class of six-strut orthogonal GSP leading to isotropy. But most of the previous works assume that the motion reference point/COM coincides with the top platform's geometric centre.

To the best of our knowledge, a general well-defined analytical solution in closed form for a dynamically isotropic MGSP is yet to be established. Though a few researchers have simplified the coupled dynamic equations for MGSP [2], their analytical expressions remain implicit and depend on multiple unknown variables that are themselves coupled. Hence, it is very tedious to calculate each of the unknowns' values and arrive a design. To overcome these problems, we have developed a geometry-based method that will give a complete closed-form solution for MGSP in an explicit form and hence can even determine the unknown radius and angle parameters easily. The above procedure was also applied to the general case, where the location of the motion reference point is not at the geometric centre of the top platform but is with some offset.

2 Formulation

A Gough-Stewart Platform (GSP) consists of a movable top platform, a fixed base, and six linearly actuated struts. In a MGSP, the anchoring points are placed at two radii on each platform as shown in Fig. 1 (a). The three struts will be of equal length, and their anchoring points are uniformly spaced along the circumference forming a 120° angle between them. The same holds for other set of three struts. We use R_{bo}, R_{bi} to denote the outer and inner radii of the bottom platform while R_{to}, R_{ti} are the outer and inner radii of the top platform, respectively. The quantity $\{x_b, y_b, z_b\}$ represents coordinates of a point on the base frame $\{B\}$ and $\{x_p, y_p, z_p\}$ denote the coordinates of a point on the top or moving frame $\{P\}$, respectively. R_{bo} is chosen along x_b, and α_{to}, α_{bi}, α_{ti} are angles made by respective radii with x_b. H is the height between the two platforms.

Compared to other methods and the use of Jacobian matrix [2,6], we use the force transformation matrix [8]. The Jacobian matrix (J) and the force transformation matrix are related for an MGSP with the force transformation matrix (B) being the transpose of an inverse Jacobian matrix [8] i.e., $B = (J^{-1})^T$. Assuming each platform as a rigid body, the stiffness matrix $[K_T]$ in the task space is given by

$$[K_T] = k[B][B]^T \tag{1}$$

where k is the elastic stiffness of the struts in the axial direction. In Fig. 1 (b), let ${}^{P}H_{c,i}$ be the height of the motion reference point (COM) with respect to the top platform, ${}^{B}t_i$ be a vector joining centers of two platforms and $S_i\,(= l_i s_i)$ be a vector along the respective leg with length l_i. Writing loop closure equation for this loop [OABP], we get

$$x_i + {}^{B}[R]_P({}^{P}p_i - {}^{P}H_{c,i}) - l_i s_i - {}^{B}b_i = 0$$

Taking the derivative with respect to time, then taking dot product with s_i and using $\dot{x}_i = v,\ \dot{s}_i = \omega_o \times s_i$, $[\dot{R}][R^T] = \omega_o \times$, we get

$$\begin{bmatrix} s_i^T & ([R]({}^{P}p_i - {}^{P}H_{c,i}) \times s_i)^T \end{bmatrix} \begin{bmatrix} v \\ \omega_o \end{bmatrix} = \dot{l}_i$$

with the definition of inverse Jacobian, $(J^{-1})\,[v \quad \omega_o]^T = \dot{l}_i$ and using $B = (J^{-1})^T$, the force transformation matrix (6×6 for MGSP) is given by

$$B = \begin{bmatrix} s_i \\ [R]({}^{P}p_i - {}^{P}H_{c,i}) \times s_i \end{bmatrix} \tag{2}$$

where $s_i = \frac{{}^{B}t_i + {}^{B}[R]_P{}^{P}p_i - {}^{B}b_i}{l_i}$.

Let $[M]$ be the payload's mass matrix in the task space, the coordinate system can be chosen to coincide with the orientation of the principal axes of the payload to obtain a diagonal structure of $[M]$ matrix without any loss of generality. If m_p is the payloads' mass and I_{xx}, I_{yy}, I_{zz} are its moment of inertia along each direction with respect to its COM, then, $[M] = diag([m_p \ m_p \ m_p \ I_{xx} \ I_{yy} \ I_{zz}])$. Our formulations are based on the neutral pose of the platform i.e., ${}^{B}[R]_P = [I]$. This is a fair assumption for operations requiring precise control such as vibration isolation and for camera pointing [1]. This also means $[B]$ and $[J]$ matrix remain constant. For the dynamic isotropy, all six eigenvalues of the natural frequency matrix must be equal. Using Eqs. (1) and (2), we can write the natural frequency matrix $[G]$ in task space as:

$$[G] = [M]^{-1}[K_T] = [M]^{-1}k[B][B]^T = \begin{vmatrix} P_{3\times3} & R_{3\times3} \\ R^T_{3\times3} & Q_{3\times3} \end{vmatrix} \tag{3}$$

$$P_{3\times3} = diag(\lambda_1,\ \lambda_2,\ \lambda_3)\ ,\ Q_{3\times3} = diag(\lambda_4,\ \lambda_5,\ \lambda_6)\ ,\ R_{3\times3} = \begin{bmatrix} \mu_{11} & -\mu_{12} & 0 \\ \mu_{12} & \mu_{11} & 0 \\ 0 & 0 & \mu_{33} \end{bmatrix}$$

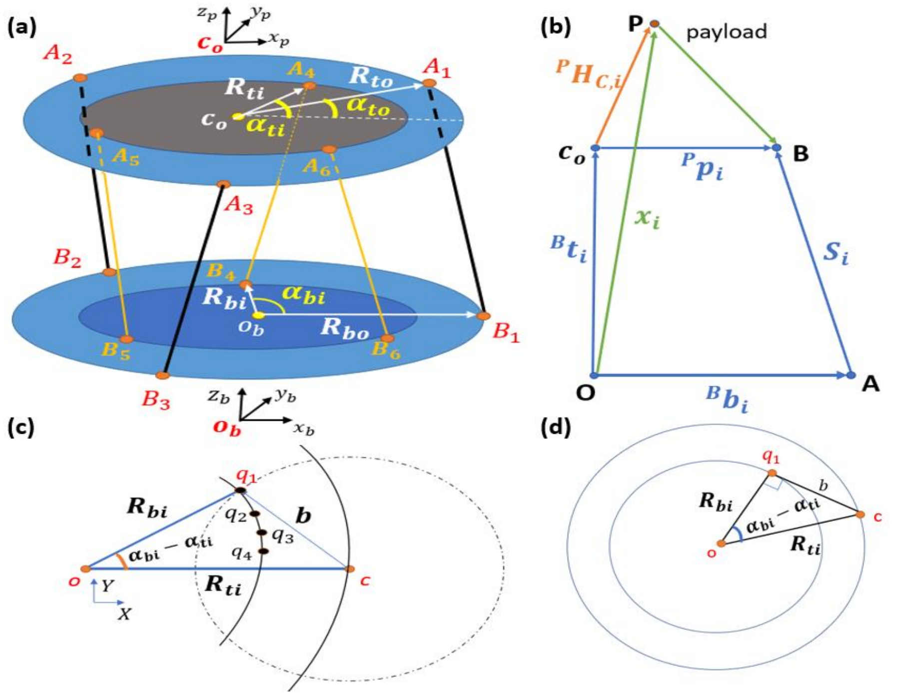

Fig. 1. a) Modified Gough-Stewart Platform b) Closed loop for MGSP c) Top view showing virtual circle and line R_{bi} intersections d) Tangency condition for virtual circle

The relation between two set of legs, with a being the leg ratio length, is given by

$$l_2 = a l_1 \tag{4}$$

where $l_1 = |S_1| = |S_2| = |S_3| = \sqrt{R_{to}^2 + R_{bo}^2 - 2R_{to}R_{bo}\cos(\alpha_{to}) + H^2}$

$l_2 = |S_4| = |S_5| = |S_6| = \sqrt{R_{ti}^2 + R_{bi}^2 - 2R_{ti}R_{bi}\cos(\alpha_{bi} - \alpha_{ti}) + H^2}$

with, ${}^B t_i = [0\ 0\ H]^T$ and ${}^P H_{c,i} = [0\ 0\ Y]^T$.

If ω denotes the natural frequency, then for complete dynamic isotropy, $\lambda_1 = \lambda_2 = \lambda_3 = \lambda_4 = \lambda_5 = \lambda_6 = \omega^2$ and $\mu_{11} = \mu_{12} = \mu_{33} = 0$. Hence, we can write

$$\lambda_1 = \frac{3k\,(l_1^2(\Psi_1) + l_2^2(\Psi_2))}{2m_p l_1^2 l_2^2}\ ,\ \lambda_2 = \frac{3k\,(l_1^2(\Psi_1) + l_2^2(\Psi_2))}{2m_p l_1^2 l_2^2}\ ,\ \lambda_3 = \frac{3kH^2(l_1^2 + l_2^2)}{m_p l_1^2 l_2^2}$$

$$\lambda_4 = \frac{3kY^2\left(l_2^2(\Psi_2) + l_1^2(\Psi_1)\right) + 6HkY\,((\Psi_3)l_1^2 + (\Psi_4)l_2^2) + 3kH^2(\Psi_5)}{2I_{xx} l_1^2 l_2^2},\ \lambda_5 = \lambda_4 \frac{I_{xx}}{I_{yy}}$$

$$\lambda_6 = \frac{3k(\Psi_6^2\, l_1^2 + \Psi_7^2 l_2^2)}{I_{zz} l_1^2 l_2^2},\ \ \mu_{11} = \frac{-3kH(-\Psi_6 l_1^2 + \Psi_7 l_2^2)}{2l_1^2 l_2^2},\ \ \mu_{33} = \frac{3kH(-\Psi_6 l_1^2 + \Psi_7 l_2^2)}{l_1^2 l_2^2}$$

$$\mu_{12} = \frac{3kH((\Psi_3)l_1^2 + (\Psi_4)l_2^2) + 3kY(l_1^2(\Psi_1) + l_2^2(\Psi_2))}{2l_1^2 l_2^2}$$

where,

$\Psi_1 = R_{ti}^2 + R_{bi}^2 - 2R_{ti}R_{bi}\cos(\alpha_{bi} - \alpha_{ti})$, $\Psi_2 = R_{to}^2 + R_{bo}^2 - 2R_{to}R_{bo}\cos(\alpha_{to})$,
$\Psi_3 = R_{ti}^2 - R_{ti}R_{bi}\cos(\alpha_{bi} - \alpha_{ti})$, $\Psi_4 = R_{to}^2 - R_{to}R_{bo}\cos(\alpha_{to})$,
$\Psi_5 = R_{ti}^2 l_1^2 + R_{to}^2 l_2^2$, $\Psi_6 = R_{ti}R_{bi}\sin(\alpha_{bi} - \alpha_{ti})$, $\Psi_7 = R_{to}R_{bo}\sin(\alpha_{to})$

3 Design of MGSP

The number of unknowns is more than the number of equations, and it is difficult to obtain a simple closed-form solutions to the above set of equations. To obtain the solution, we propose a *geometry-based method*. This is discussed below.

We start with the observation that for dynamic isotropy, $\lambda_1 = \lambda_2 = \lambda_3$ and using Eq. (4), we can get

$$b^2 = R_{ti}^2 + R_{bi}^2 - 2R_{ti}R_{bi}\cos(\alpha_{bi} - \alpha_{ti})$$

where $b^2 = \frac{H^2(3a^2+1)}{2}$ .The above equation follows the law of cosine in a triangle with sides R_{bi}, R_{ti} and b. On further extending our observation, if we project R_{ti} and α_{ti} in Fig. 1(a) to the bottom platform and visualized this from the top view, R_{bi} and R_{ti} can be seen making $(\alpha_{bi} - \alpha_{ti})$ angle between them as shown in Fig.1(c). This also comply with the same triangle and cosine rule. Hence the initial variables can be estimated using triangle, $\boldsymbol{\Delta oc q_1}$ in Fig. 1(c). For a particular height H and ratio a, variable b will be a constant. To fix this triangle, we need to find any intersection point (i.e., $q_1, q_2, q_3 \ldots$). This is basically an intersection of a *line* R_{bi} having a slope m= $tan(\alpha_{bi} - \alpha_{ti})$ ($\boldsymbol{Eq.} \rightarrow \boldsymbol{Y = mX}$) with *a virtual circle* of radius b, and center c offset by $(R_{ti}, 0)$ ($\boldsymbol{Eq.} \rightarrow \boldsymbol{(X - R_{ti})^2 + Y^2 = b^2}$), where $\{X, Y\}$ are local coordinate system at o, and X is along R_{ti} as shown in Fig.1(c).

The points q_1, q_2, q_3.. are obtained by solving for intersections at different slopes m. The solution exists when $m = \tan(\alpha_{bi} - \alpha_{ti}) \leq \sqrt{b^2/(R_{ti}^2 - b^2)}$. It can be further seen that the maximum value of m at equality corresponds to the *tangency condition*, which also implies that $\boldsymbol{\Delta oc q_1}$ is a right-angle triangle as shown in Fig.1(d). We choose this right-angle triangle case and later generalize it for other intersections.

Let $\boldsymbol{R_{ti} = x\, H}$ (note: x is a ratio which will be found later while X was an axis). Using Pythagoras theorem in $\Delta oc q_1$ in Fig. 1(d), we get

$$R_{bi} = \sqrt{x^2H^2 - b^2} = \sqrt{\left(x^2 - \frac{(3a^2+1)}{2}\right)}\, H, \text{ and } \sin(\alpha_{bi} - \alpha_{ti}) = \frac{\sqrt{\frac{(3a^2+1)}{2}}}{x}$$

The above formulation is independent of payloads' centre of mass (COM) variation Y, and remains the same for both the cases, i.e., **Case I)** Y=0 (Payload COM is on the top platform) and **Case II)** Y≠0 (Payload COM is at some offset from the top platform). We first investigate the case of Y=0 and then extend to the general case of Y≠0 and in both the cases, we aim to find the value of the variable x. The payload properties are known with $I_{xx} = I_{yy}$ a necessary condition for satisfying $\lambda_4 = \lambda_5$. This is also a valid assumption in many practical applications, especially in a symmetrical payload. Let $K = I_{xx}/I_{zz}$ and $Q = I_{xx}/m_p$, hence K and Q are known.

Case I: Closed-form solution for $\boldsymbol{Y}$=0

Using equation $\lambda_4 = \lambda_5 = \lambda_6,\ \mu_{11} = 0$ and Eq. (4), on substitutions, we get

$$R_{to} = \sqrt{\left\{2K\left(\frac{a^2+1}{a^2}\right)\left(\frac{3a^2+1}{2}\right)\left(x^2 - \frac{(3a^2+1)}{2}\right) - x^2\right\}}\ \frac{H}{a}$$

Using $\lambda_1 = \lambda_2 = \lambda_3,\ \mu_{12} = 0$ *and* Eq. (4) ,we get

$$R_{bo} = \sqrt{\left\{2K\left(\frac{a^2+1}{a^2}\right)\left(\frac{3a^2+1}{2}\right)\left(x^2 - \frac{(3a^2+1)}{2}\right) - x^2 + \left(\frac{7a^2}{2} + \frac{5}{2}\right)\right\}}\ \frac{H}{a}$$

From $\mu_{11} = 0,\ sin(\alpha_{to}) = R_{bi}R_{ti}sin\big((\alpha_{bi} - \alpha_{ti})\big)/(a^2 R_{bo}R_{to})$
From $\mu_{11} = 0,\ \mu_{12} = 0,$ and using the identity $sin^2(\alpha_{to}) + cos^2(\alpha_{to}) = 1$, on simplification, we get the value for x and then, using $\lambda_3 = \lambda_4$, we can obtain H as

$$x = \sqrt{\frac{K\,(a^2+3)\left(\frac{3a^2+1}{2}\right)^2}{K\,(a^2+3)\left(\frac{3a^2+1}{2}\right) - 2a^2}} \ \ \&\ \ H = \sqrt{\frac{Q\left(K\,(a^2+3)\left(\frac{3a^2+1}{2}\right) - 2a^2\right)}{\left\{2K\left(\frac{3a^2+1}{2}\right)^2\right\}}} \qquad (5)$$

The above solutions for H and x are in an explicit form and H can be easily chosen to satisfy our geometric constraint.

In summary, for Y=0, ***the design procedure*** involves selecting desired H from variable a and then finding x from Eq.(5) using the same a. Once H, a, and x are known, substitute them to find R_{ti}, R_{bi}, $(\alpha_{bi} - \alpha_{ti})$, R_{to}, $R_{bo,}$ α_{to} in the respective order. Also, for case a=1 (when legs are equal), it can be shown that $\boldsymbol{R_{to}} = \boldsymbol{R_{ti}}$ as shown by other reseachers after simplifications [6] which is consistent with our formulation. Fig. 2(a) and 2(b) shows plot for different parameters for a typical payload. As observed from the plots, for a=1, $R_{to} = R_{ti}$, for high value of a, R_{ti} is greater, which makes l_2 larger and for small value of a, R_{bo} is larger making l_1 larger.

We can find a general solution in this case after all the variables corresponding to the tangency condition ($a = a_o$) are known. The virtual circle (as shown in Fig.1 (c)) can be fixed keeping radius b and offset $(R_{ti}, 0)$ same as the tangency condition and all other parameters including a can change like before. The Intersection of line R_{bi} with the virtual circle for a general slope m revealed that the ***condition of tangency is the only solution***, which is evident from Fig. 2(c) where the error $(l_2 - al_1)$ is zero only at single a value for which the circle was fixed initially ($i.e.\ a_o$). Two cases for $a_o = 1$ and $\sqrt{2}$ nullify error only at $a = 1$ and $\sqrt{2}$, respectively. Multiple solutions arise from the tangency condition for different circles (different a_o values).

Case II: Solution for *Y*≠0

The calculation for variables $R_{ti},\ R_{bi}\ and\ (\alpha_{bi} - \alpha_{ti})$ remains the same as shown earlier. Taking consideration of Y now and using the same sequence as in Case I, we can write:

$$R_{to} = \sqrt{\left\{2K\left(\frac{a^2+1}{a^2}\right)\left(\frac{3a^2+1}{2}\right)\left(x^2 - \frac{(3a^2+1)}{2}\right) - \ x^2\right\}\frac{H^2}{a^2} + \frac{2Y^2(a^2+1)}{a^2}}$$

$$R_{bo} = \sqrt{R_{to}^2 + \frac{H^2}{a^2}\left(\frac{7a^2}{2} + \frac{5}{2}\right) + 4HY\left(\frac{a^2+1}{a^2}\right)}$$

Expression for calculating α_{to} remains the same as before and variable x and H can now be given as

$$x^2 = \frac{2Qa^2}{KH^2(3a^2+1)} + \frac{(3a^2+1)}{2} \qquad (6)$$

$$Y^2 + 2YH + H^2 + \frac{4Qa^2}{K(3a^2+1)^2} - \frac{Q(a^2+3)}{(3a^2+1)} = 0 \qquad (7)$$

In summary, the design procedure for ***Y*≠0** is as follows**:**

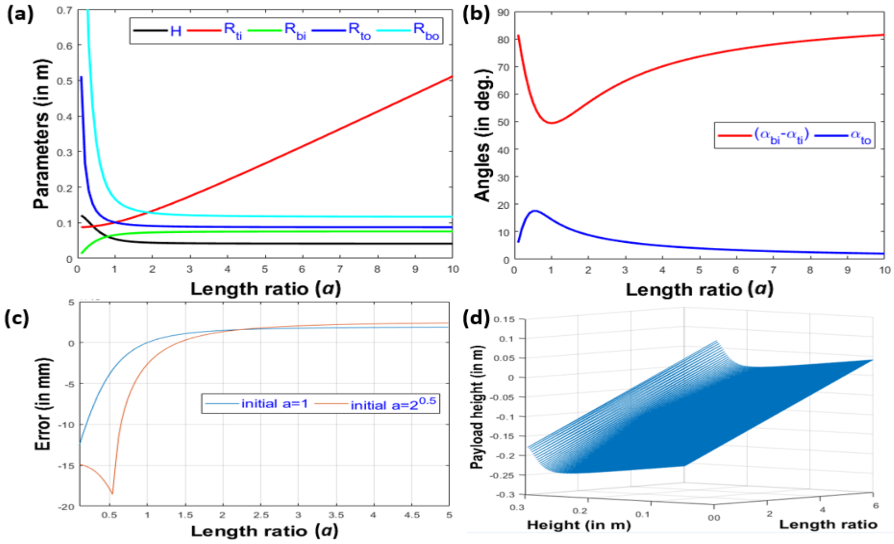

Fig. 2. a) variation of geometric parameter for case I, b) variation of angles for case I c) error $(l_2 - al_1)$ for case I for initial a i.e., a_o =1,$\sqrt{2}$ d) variation of H and Y for case II

a) Select a and H (within our constraints), from where Y and x can be obtained from Eqs (6) and (7).

b) Substitute H, Y, a, and x to find R_{ti}, R_{bi}, $(\alpha_{bi} - \alpha_{ti})$, R_{to}, $R_{bo,}\alpha_{to}$ respectively.

The variations of parameters in this case is given by Fig. 2 (d) and variation of other paramters are similar to that of case I. The inclusion of non zero Y provides more flexibility to our solution procedure and even intersections beyond tangency conditions are possible contrary to the previous case. Another interesting conclusion that can be drawn from Eq. (7) is that H and Y can be interchanged due to the equation's symmetrical nature.

In both the cases I and II, Natural frequency will depend only on k and m_p. For the dynamic isotropy, $\omega_1 = \omega_2 = \omega_3 = \omega_4 = \omega_5 = \omega_6 = \sqrt{2k/m_p}$. Hence the $[G]$ matrix will be a diagonal matrix for every solution with a diagonal value of $2k/m_p$.

4 Validation through ANSYS®

Simulations were carried out in ANSYS® with platforms treated as rigid bodies to verify the closed form solutions. The closed-form solutions were obtained for a typical payload with K =3748/6343, Q = 5.089*10^{-3} m^2, m_p = 5 Kg, and k= 10^5 N/m. Ideally, for dynamic isotropy, the ratio of the largest to the smallest natural frequency, denoted by DII, should be 1.0 and practically DII should be very close to 1. From Table 1, it can be concluded that H and Y can be interchanged, and both will have at least one dynamic isotropic configuration. The DII obtained from closed-form expression and in the simulation are very near to one (dynamic isotropic) and the natural frequency is around 31.83 Hz as obtained theoretically using $\sqrt{2k/m_p}$.

Table 1. showing DII comparison between results obtained using FEM (DII(s)) and closed-form solution (DII(t)). Here **s=FEM**, **t=theoretical** (closed-from)

Natural frequencies from ANSYS® (Configuration taken as in the closed form solution)									
(mm)	**Mode**	**1**	**2**	**3**	**4**	**5**	**6**	**DII(s)**	**DII(t)**
Y=19.2, H=35		31.68	31.70	31.73	31.81	31.82	31.84	1.005	1.00
Y=35, H=19.2		31.59	31.71	31.74	31.81	31.83	31.84	1.008	1.00

5 Conclusion

This paper deals with the design of a dynamically isotropic MGSP. Taking the variation in payloads' centre of mass and using the force transformation matrix, the natural frequency matrix was derived analytically. The closed-form solution in an explicit form was established using a *geometry-based approach* and can be used to design MGSP. For the case, when the payloads' COM is on the top platform, the tangency conditions for the virtual circle gives a complete set of solutions. When the COM is at some offset, the tangency condition is one of the solutions along with other intersection points of R_{bi} line with a virtual circle. The MGSP configurations obtained using the closed-form solution were validated via simulations using a finite element software. In future, we intend to incorporate damping and controls in our designs.

References

1. R. B. A. Shyam, N. Ahmad, R. Ranganath, A. Ghosal, "Design of a dynamically isotropic Stewart-Gough platform for passive micro vibration isolation in spacecraft using optimization", *Journal of Spacecraft Technology, December* 2019, 30(2):1-8.
2. Z. Tong, J. He, H. Jiang, G Duan, "Optimal design of a class of generalized symmetric Gough–Stewart parallel manipulators with dynamic isotropy and singularity-free workspace", *Robotica (2012)* volume 30, pp. 305–314., *Cambridge University Press 2011*.
3. J. Hong-zhou, T Zhi-zhong, He Jing-feng, "Dynamic isotropic design of a class of Gough–Stewart parallel manipulators lying on a circular hyperboloid of one sheet*", Mechanism and Machine Theory* 46 (2011), 358–374.
4. Hai Yun, L. Liu, Q. Li, W. Li, L. Tang, "Development of an isotropic Stewart platform for telescope secondary mirror", *Mechanical Systems and Signal Processing*, 127 (2019) 328–344.
5. H. Jiang, J. He, Z. Tong, W. Wang "Dynamic isotropic design for modified Gough–Stewart platforms lying on a pair of circular hyperboloids", *Mechanism and Machine Theory* 46 (2011) 1301–1315.
6. J. Yao, Y. Hou, H. Wang, T. Zhou, Y. Zhao, "Spatially isotropic configuration of Stewart platform-based force sensor", *Mechanism and Machine Theory* ,46 (2011) 142–155.
7. Y. Yi, J.E. McInroy, F. Jafari, "Generating Classes of Locally Orthogonal Gough–Stewart Platforms", *IEEE Transactions on Robotics*, vol. 21, no. 5, October 2005 812-820.
8. A. Ghosal, "ROBOTICS FUNDAMENTAL CONCEPTS AND ANALYSIS", *Oxford University Press*, February 2006.